

# Multi-scale correlations in different futures markets

M. Bartolozzi<sup>1,2</sup>, C. Mellen<sup>1</sup>, T. Di Matteo<sup>3</sup>, T. Aste<sup>3</sup>

<sup>1</sup> Research Group, Grinham Managed Funds, Sydney NSW 2065, Australia

<sup>2</sup> Special Research Centre for the Subatomic Structure of Matter (CSSM), University of Adelaide, Adelaide SA 5005, Australia

<sup>3</sup> Department of Applied Mathematics, Research School of Physical Sciences and Engineering, The Australian National University, Canberra ACT 0200, Australia

the date of receipt and acceptance should be inserted later

**Abstract.** In the present work we investigate the multiscale nature of the correlations for high frequency data (1 minute) in different futures markets over a period of two years, starting on the 1<sup>st</sup> of January 2003 and ending on the 31<sup>st</sup> of December 2004. In particular, by using the concept of *local* Hurst exponent, we point out how the behaviour of this parameter, usually considered as a benchmark for persistency/antipersistency recognition in time series, is largely time-scale dependent in the market context. These findings are a direct consequence of the intrinsic complexity of a system where trading strategies are scale-adaptive. Moreover, our analysis points out different regimes in the dynamical behaviour of the market indices under consideration.

**PACS.** Econophysics – Multiscale Phenomena – Detrended Fluctuation Analysis – Time series analysis

## 1 Introduction: persistency and anti-persistency in non-stationary systems

In recent years we have witnessed the development of a new branch of research on the edge between physics and economics. This new area, nowadays widely recognized in both the communities, goes under the name of *econophysics*. One of the most important achievement of this novel discipline has been to point out empirically that the stock market is far from being efficient: memory processes and feedbacks are present and they play a quite important role in the dynamics of this system. In particular, several studies have addressed the analysis of market fluctuations or *logarithmic returns*, defined as  $r(t) = \ln[P_r(t)/P_r(t-1)]$ , where  $P_r(t)$  is the price of a certain market at time  $t$ . Interestingly, the results show that the shape of the probability distribution function (pdf),  $P$ , irrespective of the particular stock under consideration, displays a leptokurtic behaviour<sup>1</sup>, that is “fat” tails, whose asymptotic decay can be well approximated by a power law,  $P(r) \sim r^{-\beta}$ , with exponent  $\beta \sim 3$ . This result is very important and in fact openly contrasts with the standard assumption that for a long time has ruled the academic world of theoretical economics, that is, the *efficient market hypothesis* (EMH) [3]. According to the EMH

the dynamics of market price movements are equivalent to that of white noise and, therefore, their pdf can be well represented by a Gaussian. In other words, the very large fluctuations observed in the empirical price movement distribution, and represented by the power law tails, should not exist (statistically). For a broader discussion on this subject and the field of econophysics the interested reader can refer to the books and reviews in Refs. [4,5,6,7,8,9,10].

The source of the “anomalous” behaviour in the market dynamics has to be related to *inefficiencies*, such as feedbacks in the price which, eventually, lead to very large fluctuations, such as crashes. It is obvious that the exploitation of these inefficiencies, even if for limited periods of time, becomes extremely important for traders and financial companies.

For a single asset, inefficiencies are also related to correlations in the price value over time. It is well known that first order or linear correlations can be neglected for most of the indices when looking at time scales longer than a few minutes [4,5]. This does not rule out the possibility of higher order correlations, but, in order to extract these, we need to make use of tools that are more sophisticated than the standard autocorrelation function. Moreover, we need to consider possible non-stationarities that may affect the time series: the dynamics of the stock market behaves differently according to different “environmental” conditions such as, for example, changes in the market regulation or in the trading mechanism itself.

*Detrended fluctuation analysis* (DFA), recently proposed by Peng et al. [11] in the context of DNA nucleotides

Send offprint requests to: marco.bartolozzi@gmf.com.au

<sup>1</sup> The actual shape of the distribution of returns is still a matter of debate. Intriguing frameworks have been recently proposed by Tsallis [1] and Beck [2]. A more complete discussion on this important topic is beyond the scope of the present work.

sequences, has been developed in order to extract correlations from time series with local trends - that is, from non-stationary times series. This method is particularly relevant not only to finance but also to areas such as geophysics or biophysics - where non-stationarity is the rule rather than the exception. The DFA method, summarized in Sec. 2, is based on the calculation of the average variance related to a certain trend at different scales. This procedure leads to an estimation, via a scaling relation, of the *Hurst exponent*,  $H \in [0, 1]$ , of the time series: for  $0 \leq H < 0.5$  it is said that the behaviour of the time series is *antipersistent*, and conversely, *persistent* for  $0.5 < H \leq 1$ . For completely uncorrelated movements, as assumed by the EMH, we expect  $H = 0.5$ . Note that the idea of calculating persistency/antipersistency in time series through the scaling of the variance is not peculiar to the DFA but in fact dates back to the pioneering work of Hurst (and so we obtain the name Hurst exponent) in the context of reservoir control on the Nile river dam project, around 1907 [12,13].

In the present work we investigate the temporal evolution at different scales of the *local* Hurst exponent [14, 15,16,17,18], where by the term “local” we indicate the Hurst exponent calculated at time  $t$  over a certain temporal window  $L$  that extends backward in time. This concept is very important for non-stationary and multiscale systems such as the stock market. Here, the dynamics of the trading can be influenced at different horizons by differences in the portfolio of strategies used by traders. In this case there is no reason to believe that  $H$  should remain the same for all  $t$  or that it would not vary if we calculated it using windows of a different length. For this reason the Hurst exponent is considered as “local”, in both time and length scale.

In Sec. 4 we back up the previous arguments with an empirical analysis where we show, using pdfs of local Hurst exponents, that correlations depend not only on the particular period under consideration but also on the length scale that we are observing, therefore confirming the multiscale nature of the market dynamics. Moreover, we point out how this technique can be used to monitor changes in the dynamics of the market which can be clearly observed for some specific indices.

Despite the simplicity of the previous arguments, extracting a value of the local Hurst exponent that accurately describes the serial correlation in a time series is not a trivial task. Important limitations arise from a number of different sources. A first limitation comes from the fixed temporal scale,  $L$ , that sets the limit for the number of data points to be used in the analysis. Usually a reliable estimation of  $H$  requires a large number of samples which, on the other hand, prevents the investigation of very small scales. A second limitation is related to the possible presence of non-Gaussian increments in the time series. Large non-stationary increments are able to make significant contributions to the observed value of  $H$ . In this situation the range spanned by the variance over a time interval may not be related to a sequence of temporally correlated steps in a certain direction but instead

may be primarily determined by large and possibly self-similar jumps that are temporally uncorrelated.

Furthermore, we have to consider the intrinsic precision of the algorithm used to calculate  $H$ : that has to be considered as another source of uncertainty. These issues are discussed in Sec. 3. In this regard it is important to stress that, in recent years, there has been a proliferation of methods devoted to the estimation of  $H$  or of scaling exponents in general. To the best of our knowledge each method is characterized by a unique set of advantages and disadvantages. The choice of the DFA as the working tool in the present work is related mainly to its vast popularity and, therefore, to the necessity of properly understanding its limitations. For a recent review on scaling methods in finance the interested reader could refer to [19].

The financial time series used in the analysis presented in Secs. 3 and 4, are composed of 1 minute prices for different futures contracts starting from January 2003 up until the end of December 2004. In particular we analyze:

- Stock Indices: Dax (DA), Euro Stoxx (XX), Standard & Poor500 (SP), Dow (DJ), Hang Seng (HI) and Nikkei255 (NK).
- Commodities: Gold COMEX (GC) and Crude Oil E-mini (QM).
- Exchange Rates: Japanese Yen (JY) and British Pound (BP).
- Fixed Income: Eurex Bunds (BN), Long Gilts (GL), Treasury Bonds (US) and BOBL (BL).

Each data set contains approximately  $3 \cdot 10^5$  samples, depending on the specific contract.

In summary, the present work is organized as follows: in Sec. 2 we describe the algorithm used for the calculation of the local Hurst exponent, that is the DFA. In Sec. 3, we show some possible pitfalls of this method for “fat” tailed time series by using *fractional Brownian motion* and *Lévy processes* as working examples. The main analysis is presented in Sec. 4 while discussions and conclusions are left for the last section.

## 2 The detrended fluctuation analysis method

DFA, originally proposed in Ref. [11], is considered one of the most powerful technique to extract correlations from non-stationary time series. This peculiarity makes the DFA suitable for applications to stock market time series. Some examples of its use in this field are given in Refs. [20,21,22,23,24,25,26,14,27,15,17,28,29].

The main idea behind this method is to analyze the scaling of the average fluctuations around a possible deterministic local trend of some sort. In practice, if we have a time series of random movements in time (in the same fashion as a random walk),  $x(t)$ , of total length  $N$ , which in the stock market case can be identified with the logarithmic price,  $x(t) \equiv \ln[P_\tau(t)]$ , then the implementation of the method can be summarized as following:

1. The time series is divided in  $M = N/\tau$  non-overlapping boxes of equal length  $\tau$ . In this case  $x_\tau^i(t)$  represent the sub-series of length  $\tau$  associated with the  $i^{th}$  box.

2. For each box, first we calculate the local trend which, it is assumed, can be approximate by a polynomial of degree  $p$ ,  $y_{\tau,p}^i(t)$ , and then the fluctuations,  $F^i(\tau, p)$ , around their local trend as

$$F^i(\tau, p) = \sqrt{\frac{1}{\tau} \sum_{t \in i^{th} \text{ box}} (x_{\tau}^i(t) - y_{\tau,p}^i(t))^2}. \quad (1)$$

According to the order of the polynomial used for the detrending, we indicate DFA as DFA- $p$ .

3. As the final step, the average fluctuation over the  $M$  boxes  $\langle F(\tau, p) \rangle_M = (1/M) \sum_{i=1}^M F^i(\tau, p)$  is calculated along with the  $\tau$ -scaling which, for a certain range of values, behaves as a power law

$$\langle F(\tau, p) \rangle_M \propto \tau^H. \quad (2)$$

From Eq.(2) we can finally extract the scaling exponent, for example via a linear fit over the scales where the power law holds.

Note that the accuracy of the method can be slightly influenced by the order of the polynomial used for the detrending and in principle it would be more correct to write  $H \equiv H(p)$ . However for the clarity of notation we will not write the parameter  $p$  as a variable for  $H$ . We will return to this matter in the next section where a study on the dependency of  $H$  on  $p$  has been carried out.

As mentioned in the introduction, the dynamics of the stock market can shift between phases of persistency and anti-persistency and hence there is no reason, *a priori*, to believe that the Hurst exponent has to remain constant over long periods of time. In this context it is useful to introduce the concept of *local* Hurst exponent, that is, the Hurst exponent calculated at a certain time  $t \leq N$  over a time window  $L \ll N$  which extends backwards from  $t$ . The choice of the window length  $L$  is very important from a theoretical point of view. In fact, the value of  $H$  in Eq. (2), as we will see in the next section, can change according to choice of  $L$  - hence  $L$  can be identified as a characteristic time for our calculations. The different behaviour of the Hurst exponent at different scales is nothing but an expression of the multiscale dynamics of the system enhanced by the averaged coarse-grained procedure used by the DFA algorithm when calculating the scaling relation Eq. (2). Thus the Hurst exponent at a certain temporal scale  $L_0$  can be different from the one calculated at a different scale  $L_1$ , where, for example,  $L_1 \gg L_0^2$ . In order to stress these dependencies of the parameter  $H$  we denote the local Hurst exponent calculated at a certain scale  $L$  by  $H \equiv H_L(t)$ . If we now successively shift the time window  $L$  by a discrete time lag  $\Delta t$  we are able to construct a time series of local Hurst exponents and so monitor the dynamics of the system during its evolution by extracting useful information on the correlation at a particular scale

<sup>2</sup> Note that if the EMH is realized then  $H = 0.5$  should hold independently on the particular period of time,  $t$ , or on the particular window,  $L$ , apart from numerical inaccuracies, of course.

and in a particular period of time, as shown in Figs. 6, 7 and 8 of Sec. 4.

However we are not completely free in our choice of  $L$ , being this parameter bounded by computational limitations mainly related to the minimum number of points needed to have a reliable calculation of the value of  $H$ . So far, not many studies have been devoted to this issue [30, 31] and usually, in practical applications, a rule of thumb is used. To fill this gap, in the next section we carry out an analysis devoted to investigate possible drawbacks and pitfalls of the DFA- $p$  method with variable  $L$ , in particular when applied to “fat” tailed data sets, as the case of the data investigated in the present work.

### 3 DFA: application to data sets with “fat” tails

In order to be able to perform a reliable analysis on our sets of financial data we must have an idea of the accuracy of the DFA- $p$  method under the conditions that we are going to use it.

Since we are interested in studying the changes in the correlation at short scales it would be appropriate to have an estimation of the error for small data sets. In fact, it is well known that, when dealing with power law relations such as Eq. (2), the most accurate results are achieved when a very large sample of data, spanning over several scales, is available.

Moreover, as we mentioned in the introduction, high frequency financial time series are characterized by large, non-Gaussian, fluctuations that are responsible for the “fat” tailed shape of the pdf of the returns [7]. This feature can provide an important contribution to the value of  $H$  even if there is no serial correlation (persistency/antipersistency) at all among the data. Some implications of broad tailed data in the multifractal contest and for the R/S algorithm have been discussed in Refs. [32] and [33] respectively.

#### 3.1 DFA with Gaussian increments

Before tackling the important issue of the “fat” tails and analyzing financial data, let us here give an estimation of the error associated with the calculation of  $H$  in case of Gaussian increments. In particular, we test the DFA- $p$  algorithm against an ensemble of 500 short time series ( $L = 1024$ ) of *fractional Brownian motion* (FBM) with tunable  $H$ , generated via a wavelet-construction method (WFBM) described in Ref. [34]. The average values of  $H$ , along with the standard deviations, are reported in Tab. 1 for DFA-1 and DFA-2.

The two examples give very similar results. Note that we obtain a slightly biased estimate of  $H$  for high values of correlation, ( $H \gtrsim 0.8$ ), and anticorrelation, ( $H \lesssim 0.3$ ). The systematic errors are toward smaller and larger  $H$ , respectively. However, these values are highly unrealistic for correlations in market movements where we expect to find  $H$  not too far from 0.5 (this would be different in case of

**Table 1.** Values of Hurst exponent evaluated for the WFBM with DFA-1 and DFA-2 corresponding to the nominal value reported in the first column. In both cases,  $p = 1$ , and quadratic,  $p = 2$ , polynomials to estimate the local trend. In call cases  $L = 1024$ .

	DFA-1	DFA-2
$H = 0.2$	$0.22 \pm 0.03$	$0.22 \pm 0.04$
$H = 0.3$	$0.30 \pm 0.04$	$0.31 \pm 0.04$
$H = 0.4$	$0.40 \pm 0.05$	$0.40 \pm 0.04$
$H = 0.5$	$0.50 \pm 0.06$	$0.50 \pm 0.05$
$H = 0.6$	$0.60 \pm 0.07$	$0.60 \pm 0.06$
$H = 0.7$	$0.70 \pm 0.08$	$0.70 \pm 0.06$
$H = 0.8$	$0.79 \pm 0.08$	$0.79 \pm 0.07$

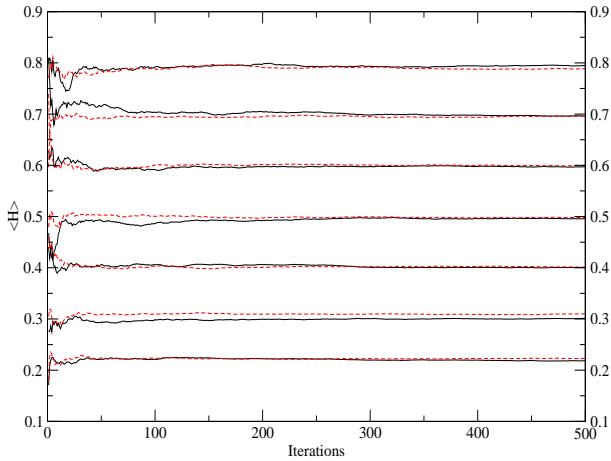


**Fig. 1.** Time series of the average value of  $H$ ,  $\langle H \rangle$ , as a function of the number of members in the WFBM ensemble, each with length  $N = 1024$ . The fact that each time series is relatively short prevents in-sample self-averaging from occurring and it actually takes the addition of a reasonable number of ensemble members before  $\langle H \rangle$  converges to a stable value. The continuous lines refer to DFA-1 while the dashed ones to DFA-2.

volatilities or volumes [23, 28, 35]). Note also that standard deviations of the DFA-2  $H$  estimates are generally smaller than that returned by DFA-1 and, therefore, we will use DFA-2 to carry out our analysis from now on. However, we must stress that the results reported in Sec. 4 are not influenced by the particular choice of  $p$ . In Fig. 1 we show the average values of  $H$  as a function of the number of members in the WFBM ensemble.

In Fig. 2 we report for DFA-2 the pdfs obtained by the previous 500 ensembles for the specific cases of  $H = 0.3$  and  $H = 0.8$ . From this plot we can clearly see the source of the bias, pointed out in the previous paragraph, as being a skewness toward 0.5 in the distributions of the evaluated Hurst exponents. Note also that if we randomly shuffle the time series, as shown in the same plot, the resulting pdfs are perfectly symmetric and centered around 0.5, as expected for uncorrelated increments. For  $0.3 \lesssim H \lesssim 0.7$ , the distributions of Hurst exponents, not shown, are Gaus-

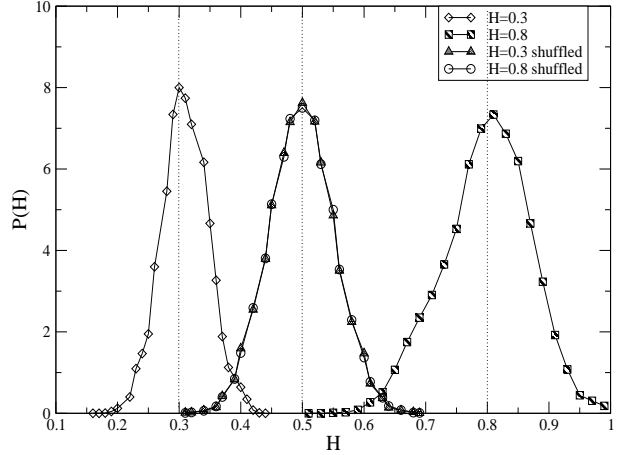


**Fig. 2.** Pdfs for  $H$  for the correlated data set of WFBM with Gaussian increments and  $L = 1024$ . As expected, the distributions for the original data sets are centered in  $H=0.3$  and  $H=0.8$ . Note also that the distributions are slightly skewed toward 0.5 leading to a slightly biased estimation of  $H$  for these high correlations - as shown also in Fig. 1. The distribution of the  $H$  values for the shuffled data is instead a Gaussian centered on 0.5. These pdfs have been averaged over 5 independent shuffling.

sian distributed and centered on the “expected” nominal value. Therefore, we can deduce that these increments do not lead any systematic bias in the DFA-2 algorithm, at least for values of  $H$  included in the range previously mentioned. In all cases the statistical uncertainty can be considered as a good estimate of the error in the  $H$  estimate. The source of the small systematic error revealed for  $H \gtrsim 0.8$  and  $H \lesssim 0.3$  is not clear - it could be in the generating process or in the estimation algorithm. It will not be considered further at this time since we are extremely unlikely to face these kinds of correlations when studying price movements. However, the source of this bias may be of interest for studies where high (low) values of the Hurst exponent are involved - such as for volatilities and volumes.

Once again using ensembles of time series produced using the WFBM method, we can try to understand how the statistical error in our estimate of  $H$  varies with  $L$ . Results from this study are plotted in Fig. 3. From this figure we deduce that the standard deviation  $\sigma_H \propto L^{-\gamma}$ , with  $\gamma \sim 0.36$ , irrespective of the particular value of  $H$  considered. This scaling law is a consequence of self-averaging effects for stationary time series. Apart from this, and as previously noticed, the absolute value of the error slightly grows with  $H$ .

### 3.2 DFA with Lévy increments

Now we turn our attention to the challenges posed by the large fluctuations which characterize high frequency financial time series. As a first step we consider the relationship

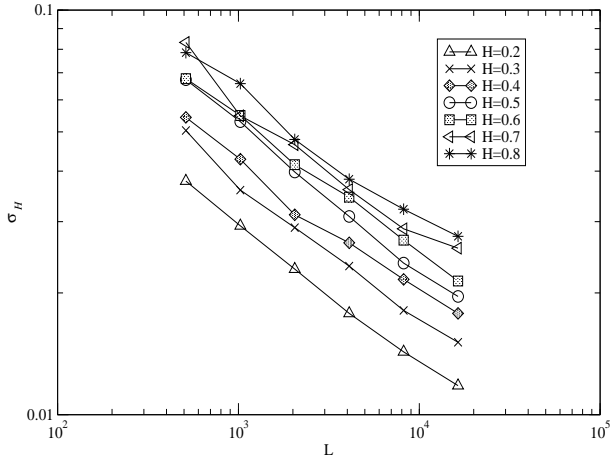


**Fig. 3.** The standard deviation of estimated  $H$  against  $L$  for Gaussian increments from the WBFM process. We can notice a power law relation with exponent  $\sim 0.36$ , independent of  $H$ . Note also that for a fixed  $L$  the standard deviation grows with  $H$ .

between the Hurst exponent and i.i.d. increments  $y$ , generated at a temporal scale  $\tau$  by a symmetric  $\alpha$ -stable Lévy process [36,6]. For  $\alpha \in (0, 2)$  the pdf of these increments is characterized by fat tails and a probability distribution

$$L_\alpha(y, \tau) \sim \frac{1}{|y|^{1+\alpha}}, \quad (3)$$

for  $y \rightarrow \pm\infty$ . As a consequence, the variance and all higher moments are infinite. Moreover, the pdf of a Lévy process obeys the scaling property

$$L_\alpha(y, \tau) = \tau^{-\frac{1}{\alpha}} L_\alpha(\tau^{-\frac{1}{\alpha}} y, 1) \equiv \tau^{-\frac{1}{\alpha}} L_\alpha^*(\tau^{-\frac{1}{\alpha}} y), \quad (4)$$

which is equivalent to saying that, irrespective of the observation scale of the process, we can always rescale the increments and the time so that every observed pdf can be collapsed into a pdf,  $L_\alpha^*$ , of rescaled increments  $\tau^{-1/\alpha} y$  and  $\tau = 1$ . This feature characterizes the statistical self-similarity of the process, despite the fact that the variables are independent.

The same feature is found for self-affine increments  $x(t)$  defined as

$$x(\lambda t) = \mu(\lambda)x(t), \quad (5)$$

to which the Hurst exponent is related<sup>3</sup> [36,37,38]. In fact, if the pdf of  $x(t)$  at certain scale  $t$  is known - say  $P(x(t), t)$  - then we can derive the corresponding pdf for the rescaled variable in  $\tau = \lambda t$ ,  $G(x(\lambda t), \lambda t)$ . From simple probability considerations we have that

$$G(y, \tau) = \left| \frac{dx}{dy} \right| P(x, t) \Big|_{y, \tau}, \quad (6)$$

where  $y = x(\lambda t)$ . It follows that

$$G(y, \tau) = \frac{1}{\mu(\lambda)} P\left(\frac{y}{\mu(\lambda)}, \frac{\tau}{\lambda}\right), \quad (7)$$

and, since the rescaling factor is arbitrary, setting  $\lambda = \tau$  gives that

$$G(y, \tau) = \frac{1}{\mu(\tau)} P\left(\frac{y}{\mu(\tau)}, 1\right) \equiv \frac{1}{\mu(\tau)} P^*\left(\frac{y}{\mu(\tau)}\right), \quad (8)$$

where  $P^*$  is the collapsing pdf with time increments  $\tau = 1$ . For mono-fractal self-affine time series the Hurst exponent is defined as  $\mu(\lambda) = \lambda^H \equiv \tau^H$ . By comparing Eq. (4) and Eq. (8) we can deduce that  $H = 1/\alpha$ . For  $0 < \alpha < 2$  we are in a fat tail regime where  $H > 0.5$  is related just to the self-affinity of the increments and not to serial correlations. Note that  $\alpha = 2$  is a special case of stable distribution, i.e., the Gaussian. In this case the Hurst exponent assumes the well known value for uncorrelated signals,  $H = 0.5$ . For an exhaustive discussion of Lévy and self-similar processes we refer the reader to the book of Samorodnitsy and Taqqu [36].

In order to validate the results presented in the previous discussion and to test the reliability of DFA-2 on Lévy processes we have performed numerical tests for different values of  $H > 0.5$  (since  $\alpha \in (0, 2)$ ) and different lengths  $L$  of the time series. The Lévy increments  $y$  have been generated via the algorithm proposed in reference [36]. Accordingly

$$y = \frac{\sin(\alpha\phi)}{[\cos(\phi)]^{1/\alpha}} \left[ \frac{\cos((1-\alpha)\phi)}{\nu} \right]^{\frac{1-\alpha}{\alpha}}, \quad (9)$$

where  $\phi$  is a uniformly distributed random number in the interval  $[-\pi/2, \pi/2]$  and  $\nu$  an independent realization of an exponential random variable with mean 1. The results for the average value of  $H$  are reported in Tab. 2 for the average obtained using 500 realizations of the Lévy process of length  $L^4$ . In this case, with the process increments being serially independent a shuffling of them would have no effect and hence all the contributions to  $H$  come from the self-similarity of the increments. Note that the accuracy of the DFA-2 algorithm in this case is quite poor. This result is not surprising at all: DFA- $p$  has been developed specifically for particular kind of trends - those that can be well described via a polynomial - and not for the large (spiky) jumps such as the ones considered in this example [39].

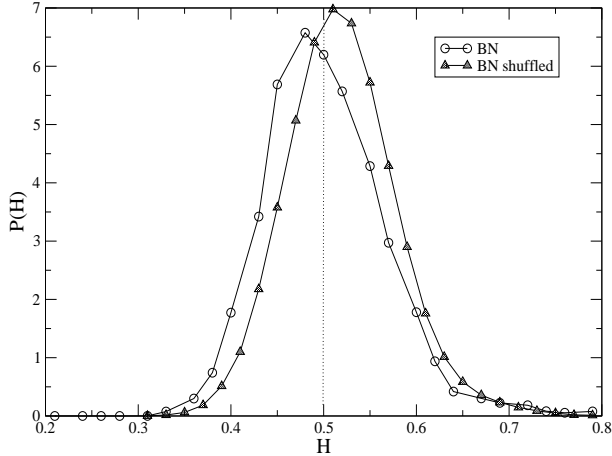
Although the tails for the Lévy stable processes tend to be systematically broader than the ones of the financial data [4,5] we can use the results from these preliminary studies as a general indication of the likely behaviour of DFA-2 when applied to “fat” tailed data. Accordingly it seems not unreasonable to expect that the presence of large non-Gaussian fluctuations in stock market data will give rise to a bias toward large  $H$ . This contribution is of no help in inferring serial correlation and, therefore, should

<sup>3</sup> Note that in Eq. (5) the equal sign holds in the statistical sense.

<sup>4</sup> Note that, since the second moment of the distribution diverges, this procedure is just limited to finite time series.

**Table 2.** Values of Hurst exponent evaluated for Lévy processes of different  $H = 1/\alpha$  and  $L$ .

	$L = 1024$	$L=4096$	$L=16384$
$H = 0.6$	$0.56 \pm 0.08$	$0.58 \pm 0.07$	$0.57 \pm 0.05$
$H = 0.7$	$0.63 \pm 0.10$	$0.64 \pm 0.08$	$0.65 \pm 0.07$
$H = 0.8$	$0.68 \pm 0.12$	$0.70 \pm 0.10$	$0.71 \pm 0.08$

**Fig. 4.** Pdfs of  $H_L(t)$  for the BN time series with  $L = 1024$ . Note that the distribution of the original data is peaked on a value slightly below 0.5. On the other side, the shuffled curve is not peaked around 0.5 but at a higher value.

be taken into consideration when drawing conclusions on the persistency/antipersistency of a time series.

### 3.3 DFA for futures indices

In this section we apply the DFA-2 to different sets of financial data. Let us start considering the logarithmic price of the 1 minute BN (Bund futures) time series. At this time scale large fluctuations are very frequent and the pdf of returns displays a pronounced leptokurtic shape. In this case, instead of producing an ensemble of short time series, we fix a time frame  $L$  and we slide it through the all the data set at intervals of 10 minutes. In addition, we applied the DFA-2 estimator to sets of shuffled BN data. The pdfs for the raw and shuffled data sets are shown in Fig. 4.

The results are quite different to those obtained from i.i.d Gaussian increments. At this scale,  $L = 1024$ , the 1 minute BN time series shows on average a slightly antipersistent behaviour. The shuffled set, on the other hand, displays a slightly persistent behaviour. This latter observation can be seen as an indication of the systematic contribution toward large  $H$  values that may be expected when large non-Gaussian fluctuations are present in the time series. Such an outcome was in fact presaged by the discussion in section 3.2. Results from the other sets of futures data show equivalent behaviour. Hence, it can perhaps be argued that if one is interested in determining  $H$

attributable to serial correlations in a data set then one should also take into account the “offset” in  $H$  that can arise from any large non-Gaussian fluctuations that may be present. This offset may be estimated by evaluating the persistency/antipersistency of the shuffled data.

In order to double check that the source of the persistence in the shuffled BN time series is related to the “fat” tails of the data set we have created a surrogate time series of the BN returns ( $r$ ) data according to

$$\begin{cases} r(t) \rightarrow |g(t)| & \text{if } r(t) > 0, \\ r(t) \rightarrow -|g(t)| & \text{if } r(t) < 0, \end{cases} \quad (10)$$

where  $g(t)$  is a random Gaussian increment. In this way, while keeping the possible temporal correlations in the increments direction, we get rid of the large fluctuations that, as we saw in the previous subsection, can be a possible source of an unwanted contribution. The results of the analysis for the BN surrogates are shown in Fig. 5. In this case, the pdf displays anticorrelation, in a similar fashion to the original time series but with a peak that is centered at a slightly lower value of  $H$ . More interesting, the Hurst exponent for the shuffled version of the surrogates is centered around 0.5 as it should be for non-correlated time series. These are important results - in fact we have shown that the value of  $H$  obtained from short leptokurtic sets is, in reality, the result of two contributions: the possible genuine temporal correlations and the self-similarity in the non-Gaussian increments, as observed for Lévy processes.

For the 1 min time series that we use in the present work we give an estimate of the average contribution to  $H$  due to the large self-similarity fluctuations: this can change from time series to time series according to their degree of intermittency. In particular we report in Tab. 3, for each index and different  $L$ , the mean value of  $H$  after shuffling the increments along with the relative difference from the theoretical value 0.5. The former can change from values of approximately 15% for the most “bursty” indices as NK, JY or BP to 2% for SP and DJ. Note also the small sensitivity on the window size for some indices. This effect is related to the phenomenon of *volatility clustering* [4,5] which enhances the value of  $H$  when smaller windows are considered.

It is important to underline that the estimate of the contribution of the large fluctuations to the value of  $H$ , see Tab. 3, is just the average effect over the two years period under consideration and cannot be directly subtracted from the single values of the  $H$  that we find. Nevertheless, it gives an idea of the order of magnitude that this phenomenon can assume, on average, over this time. A careful examination of the problem would require one to consider separately each sub-window under examination. However, the problem of manipulation of the “outliers” is not trivial: they can contain important information that otherwise could go missing. Moreover, we need to consider the multiscale nature of these fluctuations: in this context a wavelet filtering would give results appropriate for a possible analysis [40]. Part of our future work will be devoted to a further study of this problem. The problem

**Table 3.** The average values of  $H$  along with the standard deviations are reported for different indices and scales after an average over 5 independent shuffling of the time series. The relative difference,  $\Delta H/H$ , from the expected value of 0.5 is also given.

	$L = 512$	$L = 1024$	$L = 2048$	$L = 4096$	$L = 8192$	$L = 16384$	$\Delta H/H$
SP	$0.51 \pm 0.08$	$0.51 \pm 0.05$	$0.51 \pm 0.04$	$0.51 \pm 0.03$	$0.51 \pm 0.03$	$0.51 \pm 0.02$	$\approx 2\%$
DJ	$0.51 \pm 0.08$	$0.51 \pm 0.05$	$0.51 \pm 0.04$	$0.51 \pm 0.03$	$0.51 \pm 0.03$	$0.51 \pm 0.02$	$\approx 2\%$
NK	$0.58 \pm 0.10$	$0.58 \pm 0.07$	$0.57 \pm 0.05$	$0.56 \pm 0.04$	$0.56 \pm 0.03$	$0.55 \pm 0.02$	$\approx 16 \div 10\%$
HI	$0.55 \pm 0.09$	$0.55 \pm 0.06$	$0.55 \pm 0.05$	$0.54 \pm 0.04$	$0.54 \pm 0.03$	$0.53 \pm 0.02$	$\approx 10 \div 6\%$
DA	$0.52 \pm 0.09$	$0.52 \pm 0.06$	$0.52 \pm 0.04$	$0.51 \pm 0.03$	$0.51 \pm 0.03$	$0.51 \pm 0.02$	$\approx 4 \div 2\%$
XX	$0.51 \pm 0.08$	$0.51 \pm 0.05$	$0.51 \pm 0.04$	$0.51 \pm 0.03$	$0.51 \pm 0.03$	$0.51 \pm 0.02$	$\approx 2\%$
GC	$0.53 \pm 0.09$	$0.53 \pm 0.05$	$0.52 \pm 0.04$	$0.52 \pm 0.03$	$0.52 \pm 0.03$	$0.52 \pm 0.02$	$\approx 6 \div 4\%$
QM	$0.53 \pm 0.09$	$0.53 \pm 0.06$	$0.52 \pm 0.04$	$0.52 \pm 0.03$	$0.52 \pm 0.03$	$0.52 \pm 0.02$	$\approx 6 \div 4\%$
JY	$0.56 \pm 0.10$	$0.56 \pm 0.06$	$0.56 \pm 0.05$	$0.55 \pm 0.04$	$0.55 \pm 0.03$	$0.54 \pm 0.02$	$\approx 12 \div 8\%$
BP	$0.57 \pm 0.10$	$0.57 \pm 0.07$	$0.56 \pm 0.05$	$0.56 \pm 0.04$	$0.55 \pm 0.03$	$0.54 \pm 0.02$	$\approx 14 \div 8\%$
BN	$0.52 \pm 0.09$	$0.52 \pm 0.06$	$0.52 \pm 0.05$	$0.52 \pm 0.04$	$0.52 \pm 0.03$	$0.52 \pm 0.02$	$\approx 4\%$
GL	$0.52 \pm 0.09$	$0.53 \pm 0.06$	$0.53 \pm 0.06$	$0.53 \pm 0.05$	$0.53 \pm 0.05$	$0.53 \pm 0.05$	$\approx 6 \div 4\%$
US	$0.52 \pm 0.09$	$0.52 \pm 0.06$	$0.52 \pm 0.05$	$0.52 \pm 0.04$	$0.52 \pm 0.03$	$0.52 \pm 0.03$	$\approx 4\%$
BL	$0.51 \pm 0.09$	$0.52 \pm 0.06$	$0.52 \pm 0.05$	$0.52 \pm 0.04$	$0.52 \pm 0.03$	$0.52 \pm 0.03$	$\approx 4\%$

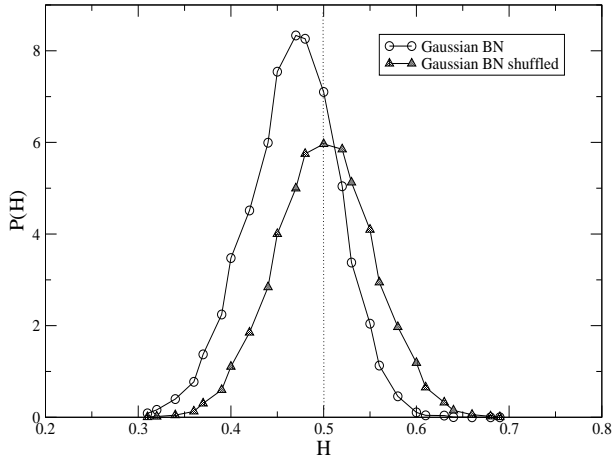


**Fig. 5.** Pdfs of  $H_L(t)$  for the surrogate BN time series with  $L = 1024$ . The distribution of the surrogate data is peaked on a value slightly smaller than the one found for the original set, underlying the positive contribution of the large fluctuations. Moreover, the shuffled version is this time centered on 0.5.

of “outliers” in the calculation of a self-affine exponents with underlying Lévy process has been addressed also in Ref. [38].

#### 4 Multiscale Hurst exponent statistics from 1/1/2003 to 31/12/2004

In this section we apply the concept of local Hurst exponent,  $H_L(t)$ , described in Sec. 2 to different future indices introduced in Sec. 1. The main aim here is to investigate its global short term statistical behaviour over the period starting from 1/1/2003 and ending 31/12/2004. The time windows used for the analysis are the following  $L = 16384, 8192, 4096, 2048, 1024$  and 512 samples which,

for the 1 minute data under consideration, span from 32 to 1 working days approximately. For lengths shorter than 512 the computation of  $H$  becomes overly contaminated by noise and therefore we take this value as our finest scale. Examples of time series of  $H_L(t)$  for some indices are shown in Figs. 6, 7 and 8 for  $L = 8192$  and a constant shift of  $\Delta t = 10$  minutes. From these figures we can notice how the Hurst exponent over  $L = 8192$  minutes is not strictly stationary during the period under consideration for any of the indices investigated. Moreover, the dynamics of  $H_L(t)$  appear to be quite different from index to index. For example, the estimates of the local Hurst exponents for the S&P500 and the Dow Jones, shown in Fig. 6, are always very close to the value of 0.5 (apart from a few periods) and, considering the estimated error over their values, there is no evidence for long periods of persistency or antipersistency at this temporal scale. A very similar situation is observed for the XX, Fig. 7 (d). Note that SP, DJ and XX are very liquid indices with large volumes involved: this is usually the case when markets are more “efficient”. These results are in agreement with the previous findings in Ref. [15].

The situation looks different for other indices: well defined periods in which  $H$  significantly differs from 0.5 can be observed. These can be due, especially for the less liquid markets and for short periods of time, to some groups of large investors that can alone actually drive the behaviour of the market.

In order to gain some insight into the general behaviour of the Hurst exponent at different scales we now calculate the pdfs of  $H_L(t)$  for various  $L$ . The results of the analysis are reported from Fig. 9 to 22.

From these plots we can infer some interesting features which characterized the multiscale dynamics of the indices under investigation during the two years period analyzed.

First of all, the various distributions, irrespective of the particular index, are all centered not too far from 0.5, as we might have expected. In fact, large deviations from this average value would have been related to significant

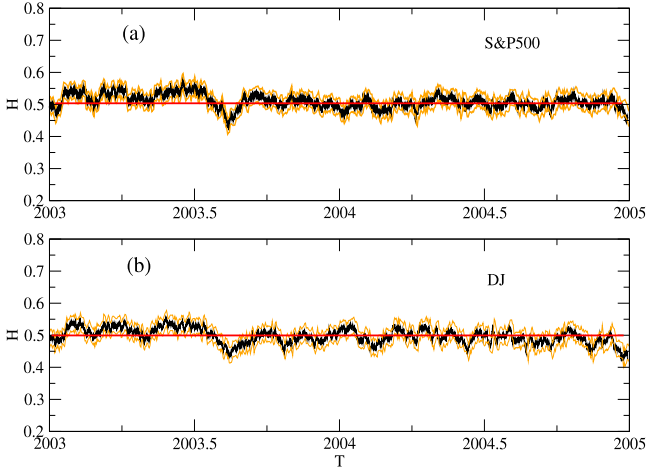


**Fig. 6.** Time series of local Hurst exponents,  $H_L(t)$ , for the time series SP (a) and DJ (b) on a scale of approximately 16 days ( $L = 8192$ ) and constant shift  $\Delta t = 10$  minutes. For these particularly liquid markets  $H$  is always very close to 0.5, irrespective of the particular scale under consideration. A confidence interval based on Gaussian errors is shown as well. The time period goes from 1/1/2003 to 31/12/2004.

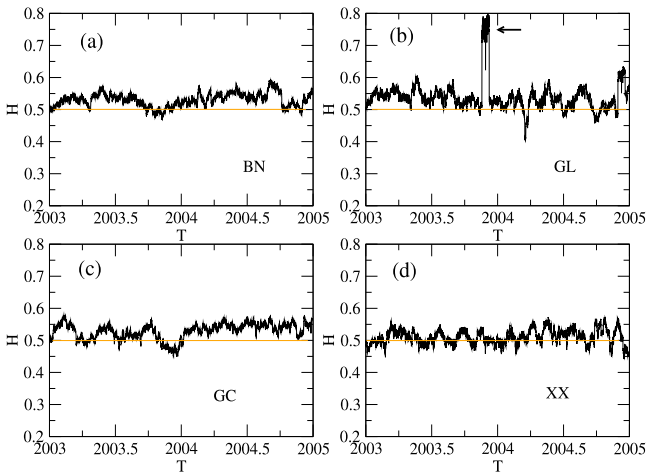


**Fig. 7.** Local Hurst exponents with  $L = 8192$  and  $\Delta t = 10$  for BN (a), GL (b) GC (c) and XX (d). The anomalous “burst” observed for GL, indicated by the arrow in (b), is nothing but an artifact of the data set where a large artificial gap is present, see also Sec. 3.

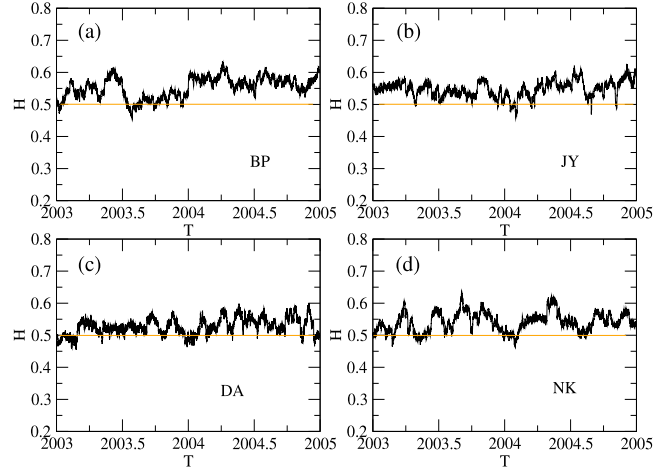


**Fig. 8.** Local Hurst exponents with  $L = 8192$  and  $\Delta t = 10$  for BP (a), JY (b) DA (c) and NK (d).

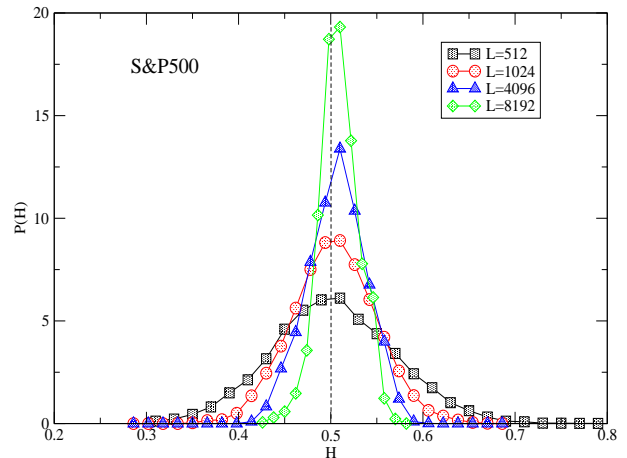


**Fig. 9.** Pdfs for  $H_L(t)$  at various  $L$  for the S&P500 futures. The distributions are peaked at  $H \sim 0.5$  for all scales considered : the index is close to “efficiency”.

inefficiencies which could have been subjected to market arbitrage. These inefficiencies do not last for long in well developed markets such as the ones studied in the present work.

As we examine the distributions in more detail we can notice that they get sharper as we increase the length of the time scale, that is, the fluctuations around the average value decrease. This is a natural consequence of the DFA-2 algorithm which produces a smaller dispersion on the



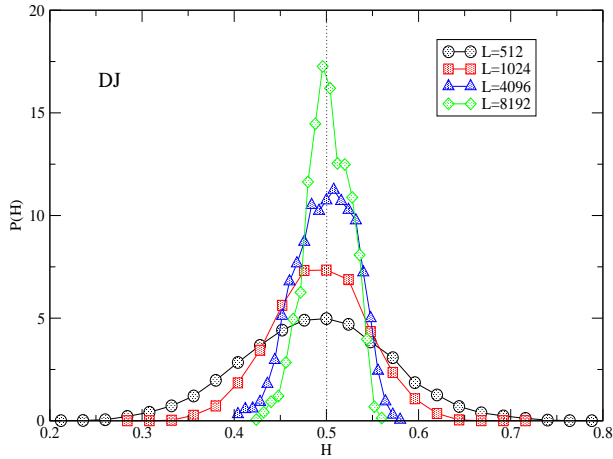


**Fig. 10.** Similarly to those of the S&P500 futures, the Dow Jones futures distributions show basically no significant correlation over the time period considered. Note the shoulder for  $L = 8192$ : this indicates a different regime in the dynamics of the system.

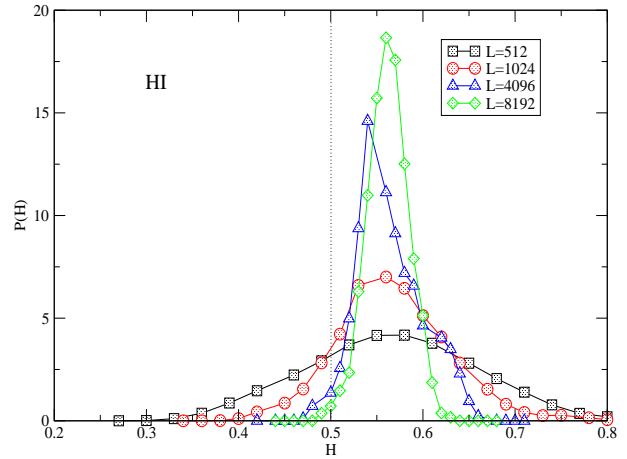


**Fig. 12.** Pdfs for the Hang Seng futures. Interestingly this is the only index where the average dynamics drifts toward a more persistent regime at shorter temporal scales.

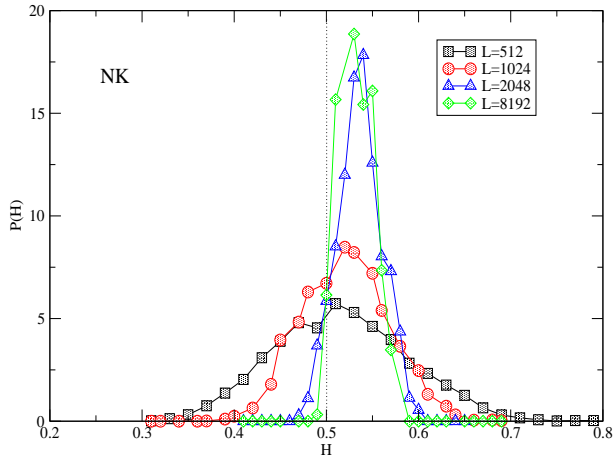


**Fig. 11.** For the Nikkei225 futures we have generally persistent behaviour with different shoulders.

value of  $H_L(t)$  as we increase the length of the time series to be evaluated.

More interestingly, a relatively smooth shift in the peak of the pdfs is evident as we move from longer to shorter scales - this is particularly noticeable for the BP, BN, QM, BL, US, GL, JY, DA and NK. Remarkably, in the BN, BL and US (fixed income) we observe a clear crossover from an average persistent to an average antipersistent dynamics at a time scale of approximately 1 day. On the other hand the HI displays a more persistent behaviour, on average, at shorter time scales.

For most of the indices there is also evidence of shoulders. These anomalies indicate that the system has moved through different phases in the period under consideration

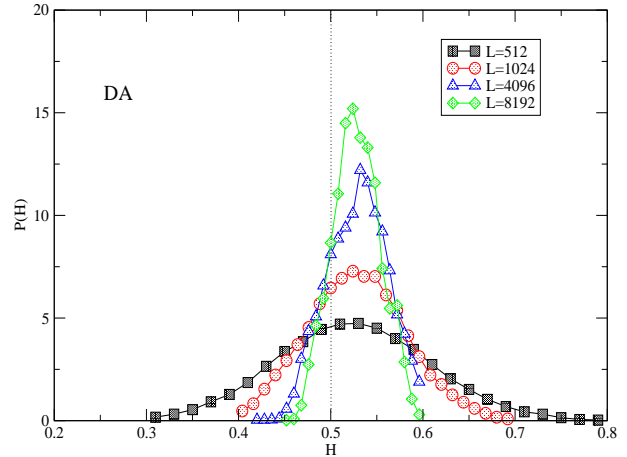


**Fig. 13.** The German DAX futures show generally persistent behaviour with some shoulders at larger scales.

and that in each phase the Hurst exponent was significantly different from its average value. This could be due to different exogenous reasons such as changes in financial regulations, market “mood” or just variations in the trading mechanism.

In order to have a feeling of how the dynamics of an index can differ over the two years period under consideration and to gain a better insight into the origin of the shoulders we split the time series of local Hurst exponent for the BP into three identical subperiods. Each of the subperiods corresponds to eight months of trading. It is clear from the relative pdfs, Fig. 23 (Top), that the dynamics of the system is rather different in each of the subperiods and it becomes clear how the shoulders have origins in these phases. Of course, this is just a pedagogical example and, in principle, we could perform a more accurate

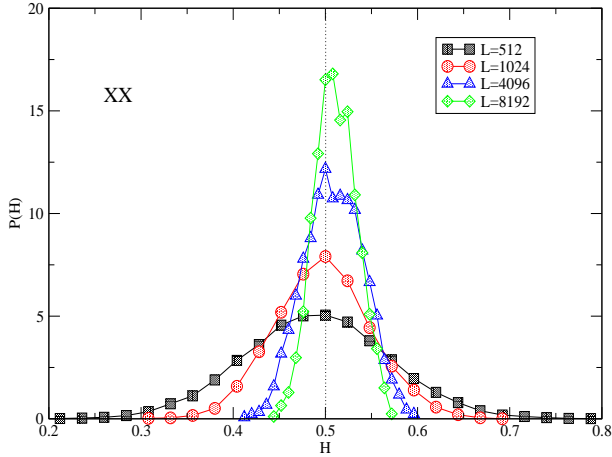


**Fig. 14.** Pdfs for the Euro Stoxx futures. No significant average correlations can be observed for the shorter scales. At the two longer scales shoulders are present for  $H > 0.5$ .

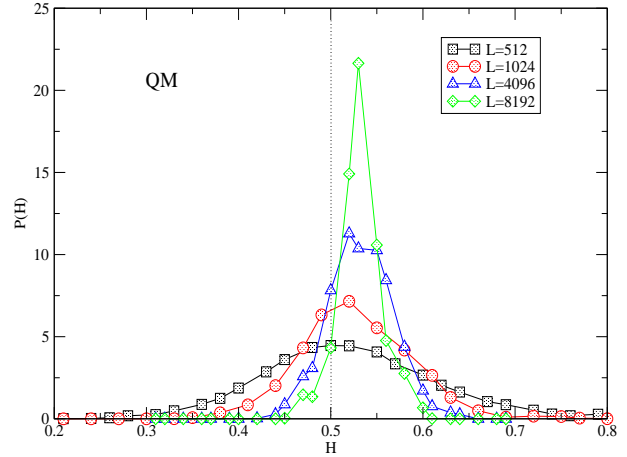


**Fig. 16.** Pdfs for the Crude Oil futures. A shift toward a “efficient” behaviour at short temporal scales can be observed.

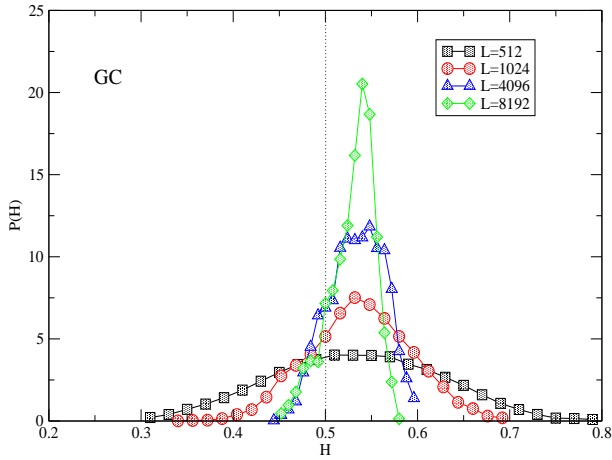


**Fig. 15.** For Gold futures we observe persistency across all scales investigated. Noticeable shoulders are present at a time scale of approximately eight working days ( $L = 4096$ ).

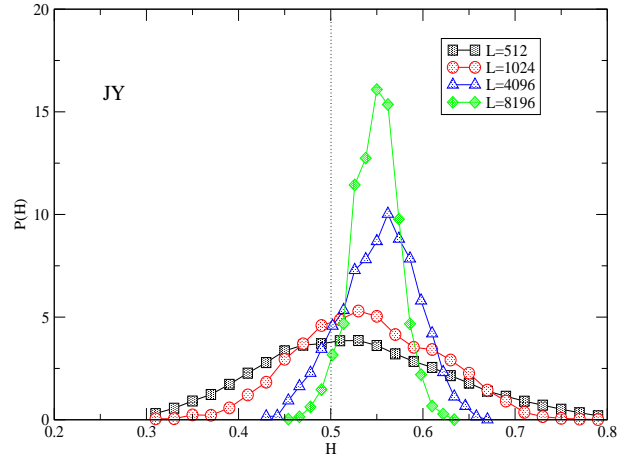


**Fig. 17.** For the Japanese Yen futures the situation is very similar to the British Pound futures, Fig. 18, where overall persistent behaviour is evident. Different changes in the dynamics are observed.

analysis by monitoring the changes in the pdf of  $H_L(t)$  in real time, as we did for the local Hurst exponent. It would be interesting, for example, to monitor the behaviour of the distribution of Hurst exponent at different scales just before a market crash. However this issue goes beyond the aim of the present paper and it will be addressed in a future work.

The relationship between the market dynamics and the scale of observation appears to become more evident when we plot the average value of the local Hurst exponent,  $\langle H \rangle_L$ , against the scale  $L$ , Fig. 24. From this graph we can notice how time series belonging to the same sector tend to have a qualitatively similar scale dependency. The indices futures, for example, Fig. 24 (a), do not display a strong correlation between  $\langle H \rangle_L$  and  $L$  with the exception

of the Hang Seng (HI) whose persistency increases sharply at smaller scales. On the other hand a scale dependency is quite evident for the fixed income products, Fig. 24 (d), where, interestingly, some time series (BN, US and BL) move from an antipersistent-like to an persistent-like behaviour as the scale increases, as already pointed out by our qualitative observation of the pdfs.

As a result of the analysis carried out in this section we can claim that the actual behaviour of the stock market, described in terms of Hurst exponent, apart from being influenced by the particular period of time under consideration and by the maturity of the market [15,41,16,42, 43], is also related to the particular scale of observation: this is an extremely relevant issue for practical applications. In fact, if we consider long time scales (large  $L$ ), in

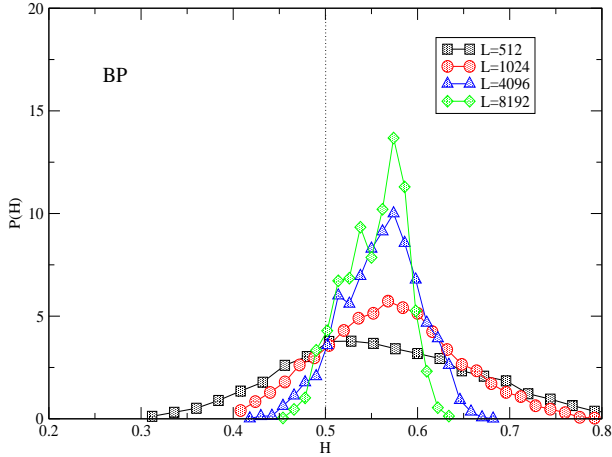


**Fig. 18.** The British Pound futures display generally persistent behaviour interrupted by many shoulders: different phases have characterized the two years period considered.

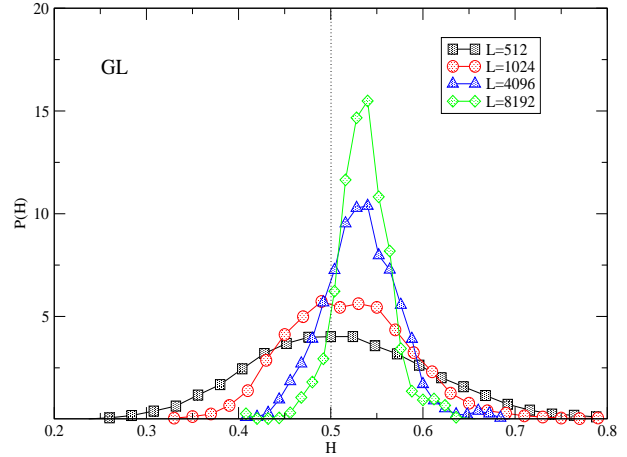


**Fig. 20.** The pdfs for the Long Gilts futures point out an average slightly persistent behaviour until a time frame of approximately one trading day ( $L = 512$ ). Shoulders are present as well.

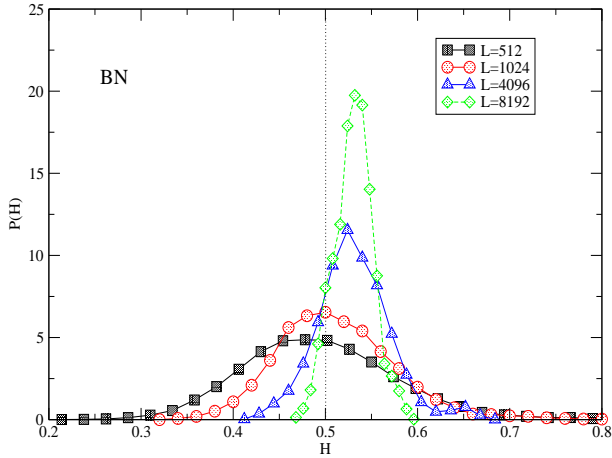


**Fig. 19.** The pdfs for the Eurex Bunds futures show a quite singular behaviour. The index seems to shift from a slightly persistent to a slightly antipersistent behaviour as we move toward smaller scales.

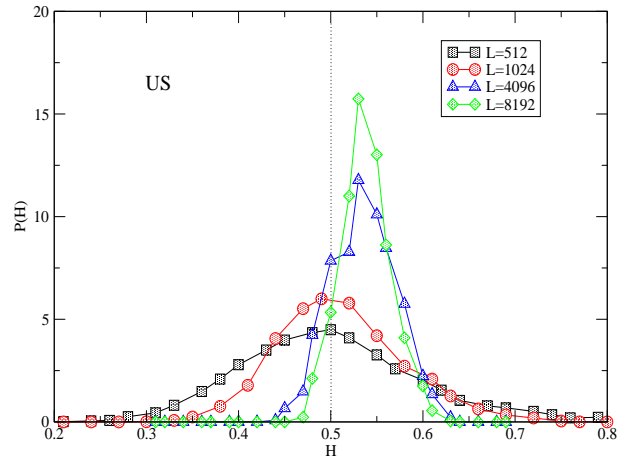


**Fig. 21.** Pdfs for the Treasury Bonds futures. A smooth shift toward antipersistence at short time scales can be observed.

reality, we are estimating the *average* Hurst exponent over that period.

Moreover, these empirical findings confirm the multi-scale and non-stationary nature of the stock market, in contrast with the assumptions inherent in the EMH.

#### 4.1 Hurst exponent and end-of-day gaps

Before concluding, we want also to briefly address the question of the relevance of end-of-day (EOD) gaps in the analysis carried out so far. It is well known that the price can undergo large changes while a market is not in session. This phenomenon is mainly related to the flow of

information from active markets in different time zones which, somehow, is “digested” by other markets during their closure and then reflected in the opening price of the following day.

So far we have considered these changes as a natural part of the dynamics of the market itself. In this last section, instead, we want to consider the relative importance of these events in our analysis by treating them as “spurious” effects. In fact, as we already discussed, large fluctuations tend to increase the value of the Hurst exponent despite the genuine presence of persistency in the time series. In order to account for this fact we have removed from the original time series the EOD returns and then we have repeated the analysis performed in the previous section. A summary of the results for the average

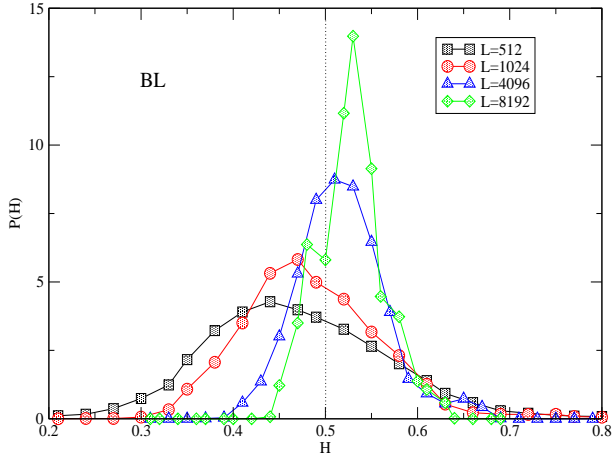


Fig. 22. Pdfs for the BOBL futures. As for the Bunds, Fig. 19 a succession from persistency to antipersistency is evident

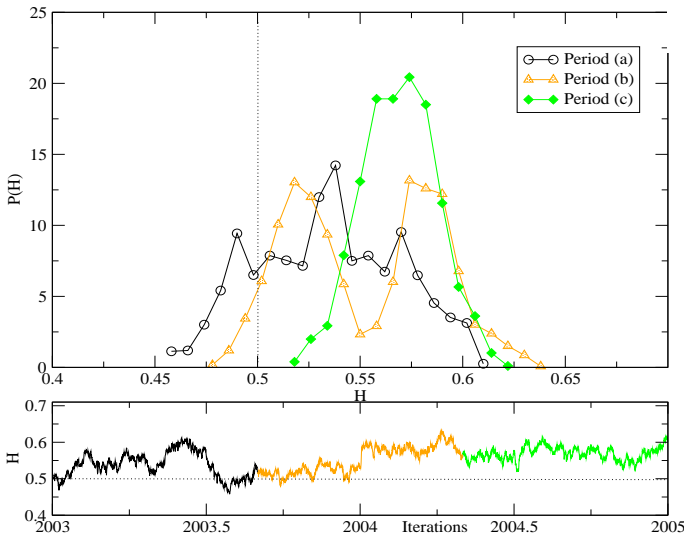


Fig. 23. (Top) Pdfs of three subperiods, (Bottom), for the BP. Note the different distributions of the Hurst exponent: these are clear indications of non-stationarity in the time series. In this plot we used  $L = 8192$ .

value of  $H_L(t)$  is shown in Fig. 25. If we compare these plots with Fig. 24 we can notice how most of the curves, while maintaining the same qualitative shape, are shifted toward smaller values of  $\langle H \rangle$ , as expected.

However, it is important to point out how this shift can change the conclusions of the analysis in terms of persistency/antipersistency. For example, the exchange rates futures appear to move from an average persistent behaviour at all scales, Fig. 24 (c), to an average uncorrelated behaviour for the BP and anticorrelated for the JY, Fig. 25 (c).

This last analysis, therefore, confirms the relevance of the large fluctuations in the calculation of Hurst exponents. Moreover, it points out the issue of the preconditioning of high frequency data: this can lead to dif-

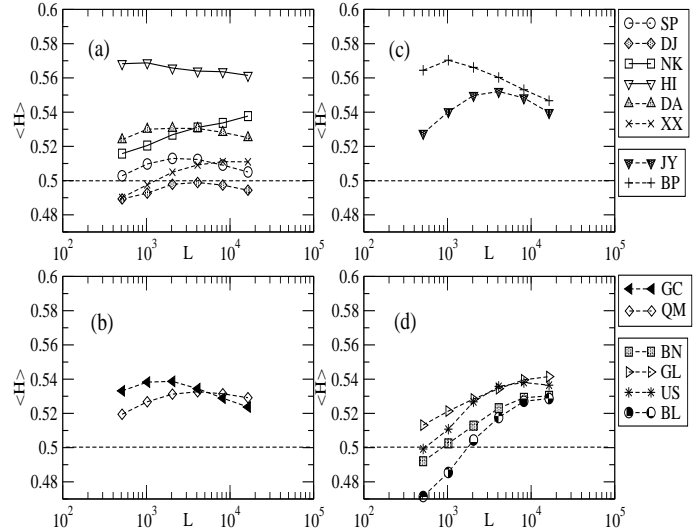


Fig. 24. Average value of the local Hurst exponent,  $\langle H \rangle_L$ , for index futures (a), commodity futures (b), exchange rate futures (c) and fixed income futures (d). The error bars on these points, not plotted for clarity, are approximately equal to the standard deviations in Tab. 3. The horizontal dotted line is set at 0.5 for visual reference.

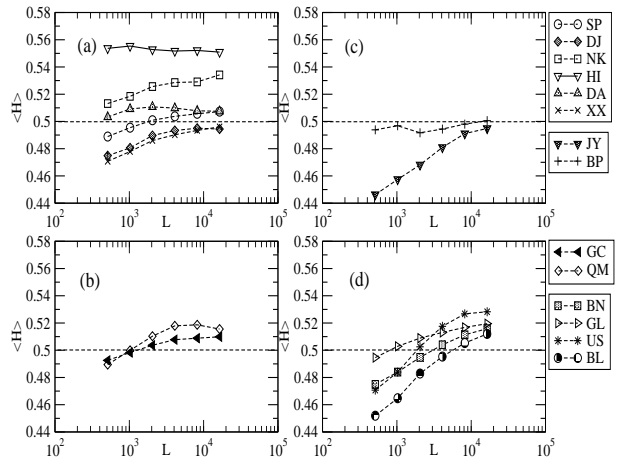


Fig. 25. Same as Fig. 24 but, this time, in the analysis we do not consider price returns that cross two different days.

ferent conclusions regarding their behaviour across time series.

## 5 Discussion and conclusion

In the present work we have used the concept of local Hurst exponent in order to investigate the short scale dynamical properties of the correlations in different future contracts (indices, commodities, exchange rate and fixed income) from the beginning of 2003 to the end of 2004.

Analysis on the behaviour of  $H_L(t)$  at different scales, and in particular its distribution, points out a scale dependent and non-stationary evolution of this scaling exponent, independent of the specific kind of contract.

The Eurex Bunds, BOBL and U.S Treasury Bonds, for example, display an average persistent behaviour over time scales of approximately three weeks but they then become antipersistent, on average, for time scales of the order of one day. Moreover, we observe changes in the shape of the pdfs of  $H_L(t)$  with time. This fact points to the existence of different market phases in the two years period from 1/1/2003 to 31/12/2004 and, therefore, evidence for non-stationarity. These empirical facts are in contrast with the EMH hypothesis, according to which  $H_L(t)$  should be constant and equal to 0.5 for each time scale.

It is worth to stress that the dynamical behaviour of the Hurst exponent is not related only to the liquidity of the market but also to the variety of time horizons involved in the trade of a particular asset. As a consequence, markets which involve many exogenous agents, such as the S&P500, tend to be more “efficient”.

In conclusion, we have shown that the concept of Hurst exponent for non-stationary time series has a practical validity only in the period and the scale of observation. By estimating  $H$  with a large sample, due to the coarse-grain procedure of the DFA- $p$  algorithm, we lose the local information and we obtain an “average” value over that period. This can or cannot be a problem for technical trading: it depends on the horizon we are interested in. Moreover, market models should be bounded to reproduce the time-scale variability of the Hurst exponent, as already pointed out in Ref. [15].

In addition, we have shown that self-similarity of the large fluctuations responsible for the “fat” tail property of financial time series can produce a substantial contribution to the value of  $H$  which is not related to temporal correlations in the price variation. This effect cannot be neglected for high frequency financial applications or, in general, for “fat” tailed data sets. In particular, we have pointed out the contribution of the EOD gaps present in high frequency financial data. These results are in agreement with the conclusions of Alfi et al. [33] who investigated the robustness of the R/S algorithm [12] against tick-by-tick data from the New York Stock Exchange. Note, however, that the DFA- $p$  algorithm results to be more robust than the R/S method with respect to both the large fluctuations and the window size. In particular, for small samples and Gaussian increments, we do not observe the systematic bias of  $H$  that was reported in [33] - at least for  $0.3 \lesssim H \lesssim 0.8$  (see Sec. 3.1 for details).

Given the present results we feel it will be necessary to develop an alternative methodology - one that is not based on scaling exponents - if we are to reliably exploit the high order correlations found in non-stationary and fat tailed data sets. Some alternatives could be found in random matrix theory [44,45,46], hyperbolic networks [47], or information theory tools such as the transfer entropy [48].

Finally, it is worth noting that the time/scale dependency of the scaling exponent  $H$  investigated in the present work can also be extended to the multifractal framework [32]. In this case, the time series is assumed to be characterized not by one but by an entire spectrum of scaling exponents. Our future work will be devoted to the study of the temporal properties of these multifractal spectra in different financial time series [49,50,51,52,53,19] along with their financial implications.

## Acknowledgement

The authors would like to thank Richard Grinham for many useful discussions and a careful reading of the manuscript. TDM and TA acknowledge the partial support by ARC Discovery Projects: DP03440044 (2003) and DP0558183 (2005), COST P10 “Physics of Risk” project and M.I.U.R.-F.I.S.R. Project “Ultra-high frequency dynamics of financial markets”.

## References

1. C. Tsallis, C. Anteneodo, L. Borland and R. Osorio, *Physica A* **324**, 183 (2003).
2. C. Beck and E. G. D. Cohen, *Physica A* **322**, 189 (2002).
3. M.M. Dacorogna, U.A. Müller, R.B. Olsen and O.V. Pictet, *Quant. Finan.* **1**, 198 (2001).
4. R.N. Mantegna and H.E. Stanley, *An Introduction to Econophysics: Correlation and Complexity in Finance*, (Cambridge University Press, Cambridge, 1999).
5. J.-P. Bouchaud and M. Potters, *Theory of Financial Risk and Derivative Pricing: from Statistical Physics to Risk Management*, (Cambridge University Press, Cambridge, 1999).
6. W. Paul and J. Baschnagel, *Stochastic Processes: From Physics to Finance*, (Springer-Verlag, Berlin,1999).
7. M.M. Dacorogna, R. Gençay, U.A. Müller, R.B. Olsen and O.V. Pictet, *An Introduction to High-frequency Finance*, (Academic Press, San Diego, 2001).
8. J. Feigenbaum, *Rep. Prog. Phys.* **66**, 1611 (2003).
9. *Proceedings to the international conference “Econophysics Colloquium”*, *Physica A* **370** (1) (2006).
10. “*Topical Issue: Trends in Econophysics*”, *Eur. Phys. J. B* **55** (2) (2007).
11. C.-K. Peng et al., *Phys. Rev. E* **49**, 1685 (1994).
12. J. Feder, *Fractals*, (Plenum Press, New York & London, 1988).
13. H. Hurst, *Trans. Amer. Soc. Civil Eng.* **116**, 770 (1951).
14. S.V. Muniandy, S.C. Lim and R. Murugan, *Physica A* **301**, 407 (2001).
15. R.L. Costa and G.L. Vasconcelos, *Physica A* **329**, 231 (2003).
16. D.O. Cajueiro and B.M. Tabak, *Physica A* **336**, 521 (2004).
17. D. Grech and Z. Mazur, *Physica A* **336**, 133 (2004).
18. A. Carbone, G. Castelli and H.E. Stanley, *Physica A* **344**, 267 (2004).
19. T. Di Matteo, *Quant. Finan.* **7**(1), 21 (2007).
20. P. Cizeau, Y.H. Liu, M. Meyer, C.K. Peng and H.E. Stanley, *Physica A* **245**, 441 (1997).

21. Y.H. Liu, P. Cizeau, M. Meyer, C.K. Peng and H.E. Stanley, *Physica A* **245**, 437 (1997).
22. N. Vandewalle and M. Ausloos, *Physica A* **246**, 454 (1997).
23. Y. Liu, P. Gopikrishnan, P. Cizeau M. Mayer, C.-K. Peng Phys. and H.E. Stanley, *Rev. E* **60**, 1390 (1999).
24. I.M. Jánosi, B. Janecsó and I. Kondor, *Physica A* **269**, 111 (1999).
25. P. Gopikrishnan, V. Plerou, Y. Liu, L.A.N. Amaral, X. Gabaix and H.E. Stanley, *Physica A* **287**, 362 (2000).
26. P. Gopikrishnan, V. Plerou, X. Gabaix, L.A.N. Amaral and H.E. Stanley, *Physica A* **299**, 137 (2001).
27. K. Matia, L.A.N. Amara, S.P. Goodwin and H.E. Stanley, *Phys. Rev. E* **66**, 045103(R) (2002).
28. P. Ivanov, A. Yuen, B. Podobnik and Y. Liu, *Phys. Rev. E* **69**, 56107 (2004).
29. Z. Eisler and J. Kertész, *cond-mat/0606161* (2006).
30. R. Weron, *Physica A* **312**, 285 (2002).
31. L. Xu, P. Ivanov, K. Hu, Z. Chen, A. Carbone and H.E. Stanley, *Phys. Rev. E* **71**, 051101 (2005).
32. J.W. Kantelhardt et al., *Physica A* **316**, 87 (2002).
33. V. Alfi, F. Coccetti, A. Petri and L. Pietronero, *Eur. Phys. J. B* **55**, 135 (2007).
34. P. Abry and F. Sellan, *Appl. and Comp. Harmonic Anal.* **3**, 377 (1996).
35. Z. Eisler and J. J. Kertész, *Eur. Phys. J. B* **51**, 145 (2006).
36. G. Samorodnitsky and M.S. Taqqu, *Stable non-Gaussian Random Processes: Stochastic Models with Infinite Variance*, (Chapman & Hall, New York, 1994).
37. P.A. Groenendijk, A. Lucas and C.G. de Vries, *Preprint of Erasmus University* **1**, 1 (1998) (<http://www.few.eur.nl/few/people/cdevries/>).
38. K. Kiyani, S.C. Chapman and B. Hnat, preprint: *physics/0607238*.
39. K. Hu, P. Ivanov, Z. Chen, P. Carpena and H.E. Stanley, *Phys. Rev. E* **64**, 011114 (2001).
40. M. Bartolozzi, D.B. Leinweber and A.W. Thomas, *Physica A* **370**, 132 (2006).
41. T. Di Matteo, T. Aste and M.M. Dacorogna, *Physica A* **324**, 183 (2003).
42. T. Di Matteo, T. Aste and M.M. Dacorogna, *Journal of Banking & Finance* **29**(4), 827 (2005).
43. R. Liu, T. Lux and T. Di Matteo, *Physica A* **383**, 35 (2007).
44. S. Drożdż, J. Kwapien, F. Grümmer, F. Ruff and J. Speth, *Physica A* **299**, 144 (2001).
45. V. Plerou, P. Gopikrishnan, B. Rosenow, L.A.N. Amaral, T. Guhr and H.E. Stanley, *Phys. Rev. E* **65**, 066126 (2002).
46. M. Potters, J.-P. Bouchaud and L. Laloux, preprint: *ArXiv:physics/0507111*.
47. M. Tumminello, T. Aste, T. Di Matteo and R.N. Mantegna, *PNAS* **102**(30), 10421 (2005).
48. R. Marschinski and H. Kantz, *Eur. Phys. J. B* **30**, 275 (2002).
49. J.-P. Bouchaud, M. Potters and M. Mayer, *Eur. J. Phys. B* **13**, 595 (2000).
50. T. Lux, *Quant. Fina.* **1**, 632 (2001).
51. L. Calvet and A. Fisher, *Rev. Econ. Statist.* **84**, 381 (2002).
52. T. Lux, *Int. J. Mod. Phys. C* **15**, 481 (2004).
53. L. Borland, J.-P. Bouchaud, J.-F. Muzy and G. Zumbach, preprint: *cond-mat/0501292*.